Weed Science

www.cambridge.org/wsc

Herbicidal activity and molecular docking study of novel PPO inhibitors

Li-Xia Zhao[1,*], Mao-Jun Jiang[2,*], Jia-Jun Hu[2], Yue-Li Zou[3], Shuang Gao[4], Ying Fu[5] and Fei Ye[5]

[1]Associate Professor, Department of Applied Chemistry, College of Science, Northeast Agricultural University, Harbin, China; [2]Master's Degree Student, Department of Applied Chemistry, College of Science, Northeast Agricultural University, Harbin, China; [3]Senior Experimentalist, Department of Applied Chemistry, College of Science, Northeast Agricultural University, Harbin, China; [4]Associate Professor, Department of Applied Chemistry, College of Science, Northeast Agricultural University, Harbin, China and [5]Professor, Department of Applied Chemistry, College of Science, Northeast Agricultural University, Harbin, China

Research Article

Cite this article: Zhao L-X, Jiang M-J, Hu J-J, Zou Y-L, Gao S, Fu Y, Ye F (2020) Herbicidal activity and molecular docking study of novel PPO inhibitors. Weed Sci. **68**: 565–574. doi: 10.1017/wsc.2020.66

Received: 1 March 2020
Revised: 17 July 2020
Accepted: 20 August 2020
First published online: 28 August 2020

Associate Editor:
Dean Riechers, University of Illinois

Keywords:
Biological activity; diphenyl ether; tetrahydrophthalimide

Authors for correspondence:
Ying Fu, Department of Applied Chemistry, College of Science, Northeast Agricultural University, Harbin 150030, China. (Email: fuying@neau.edu.cn); and
Fei Ye, Department of Applied Chemistry, College of Science, Northeast Agricultural University, Harbin 150030, China. (Email: yefei@neau.edu.cn)

*These authors contributed equally to this work.

© The Author(s), 2020. Published by Cambridge University Press on behalf of the Weed Science Society of America.

Abstract

Protoporphyrinogen oxidase (PPO) is an important target for discovering new herbicides that interfere with the synthesis of porphyrin. To discover new PPO inhibitors with improved biological activity, a series of new diphenyl ethers containing tetrahydrophthalimide were designed and synthesized. Among them, J6.1 ($IC_{50} = 4.7$ nM) and J6.3 ($IC_{50} = 30.0$ nM) show higher maize (*Zea mays* L.) PPO inhibitory activity than the commercial herbicides oxyfluorfen ($IC_{50} = 117.9$ nM) and flumioxazin ($IC_{50} = 157.1$ nM). The greenhouse herbicidal activity of J6.3 is comparable to that of oxyfluorfen, and it is greater than that of flumioxazin. Even at a dose of 300 g ai ha^{-1}, cotton (*Gossypium hirsutum* L.) and peanut (*Arachis hypogaea* L.) show greater tolerance to J6.3, suggesting that J6.3 could be used for further development of new herbicide candidates in those fields. In addition, molecular docking has been used to further study the mechanism of action of J6.3. The results show that the introduction of a nitro group and tetrahydrophthalimide into the diphenyl ether structure is beneficial to biological activity.

Introduction

In recent years, the widespread use of glyphosate has led to the emergence of various glyphosate-resistant weeds (Alcantara-de la Cruz et al. 2019; Heap and Duke 2018; Powles 2008; Schryver et al. 2017). As a result, protoporphyrinogen oxidase (PPO) inhibitors have garnered significant interest due to their ability to effectively control glyphosate-resistant weeds (Dayan et al. 2018; Kaur et al. 2014). Furthermore, PPO inhibitors have several attractive advantages: low application rates, broad herbicidal activity, low environmental impact, and low toxicity to mammals (Wang et al. 2017). The underlying mechanism of PPO-inhibiting herbicides is interference with the synthesis of porphyrins in a plant. This inhibition of PPO activity results in the accumulation of the enzyme product protoporphyrin IX in the cytoplasm. Once protoporphyrin IX is exposed to light, it reacts with oxygen to produce large amount of reactive oxygen species. These reactive oxygen species, in turn, can damage plant cell membranes and rapidly causing symptoms related to plant burn within 1 d (Dayan and Dayan 2011; Duke et al. 1991; Qin et al. 2010; Wang et al. 2013).

Over the past 60 yr, various types of PPO inhibitors have been introduced in the market, such as diphenyl ethers, phenylpyrazoles, oxadiazoles, triazolinones, thiadiazoles, pyrimidineones, oxazolidinediones, isoxazoles, and *N*-phenyl phthalimides (Jiang et al. 2011; Wang et al. 2019). Among them, diphenyl ether is the most popular PPO-inhibiting herbicide due to its excellent herbicidal activity. As early as 1963, the first diphenyl ether PPO-inhibiting herbicide was introduced to the market by Dow AgroScience. Subsequently, several agrochemical companies have begun to conduct in-depth research on such structures, and they have discovered a variety of highly active diphenyl ether compounds. As shown in Figure 1, oxyfluorfen, fluoroflycofen-ethyl, and lactofen have been successfully commercialized. However, the frequent repeated usage of these herbicides has led to the emergence of resistant weeds (Dayan et al. 2018; Ye et al. 2019b). In addition, these herbicides have poor selectivity in crops (Yu et al. 2011). Therefore, it is necessary to modify the structure of such herbicides.

Interestingly, another type of PPO-inhibiting herbicide, *N*-phenylphthalimide, is a highly selective and rapidly degrading herbicide. For example, flumioxazin is a PPO-inhibiting herbicide that can be used for weed control in a various crops such as soybean [*Glycine max* (L.) Merr.], peanut (*Arachis hypogaea* L.), and fruit trees (Ucles et al. 2018; Yang 2001). According to the relevant literature reports, the main degradation mechanism of flumioxazin is first the cleavage of the imide ring, and then it gradually decomposes into the corresponding bound residues (Figure 2) (Shibata et al. 2011). Therefore, the tetrahydrophthalimide structure

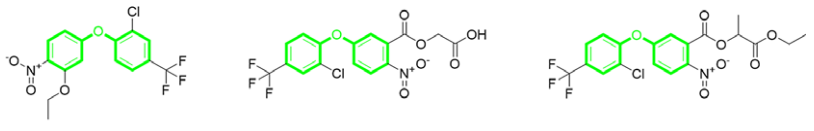


Figure 1. Representative diphenyl ether herbicides.

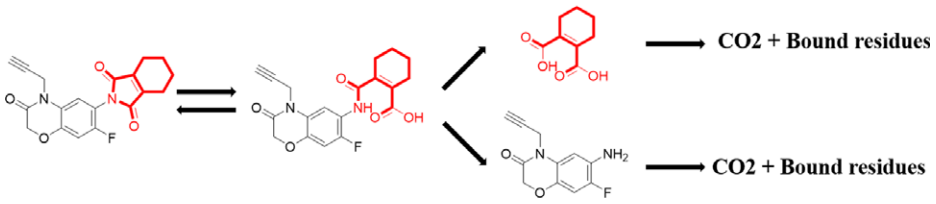


Figure 2. Degradation pathway of flumioxazin.

of *N*-phenylphthalimide herbicide has the advantage of improving the degradability and crop tolerance of the compound. Moreover, substructure splicing is a widely used method in the discovery of new drugs. In the development of pesticides, many potential lead compounds are designed based on this method (Gao et al. 2020; Ye et al. 2019a, 2019b; Zhang et al. 2020a). These findings have inspired us to introduce tetrahydrophthalimide structures into diphenyl ether herbicides, which could lead to the discovery of new herbicides with high activity, enhanced safety, and low residue levels (Figure 3).

In this current work, a series of diphenyl ether derivatives containing the tetrahydrophthalimide structure were synthesized. All the synthesized compounds were characterized using high-resolution mass spectrometry (HRMS) and nuclear magnetic resonance spectroscopy (NMR). In addition, experiments involving in vitro enzyme activity on maize (*Zea mays* L.) PPO, greenhouse herbicidal activity, crop tolerance, molecular docking, and herbicidal activity against resistant weeds were carried out using the series of compounds synthesized. Based on the observation of these experimental results, the structure–activity relationships (SARs) of these compounds are also discussed in this work.

Materials and Methods

Reagents and Analysis

All chemical reagents, such as 4-chloro-3-nitrobenzoic acid, 3,5-dimethylphenol, 3,4,5,6-tetrahydrophthalic anhydride, and thionyl chloride were purchased from Aladdin Reagent (Shanghai, China). Organic solvents, such as ethyl acetate, petroleum ether (bp 60 to 90 C), dichloromethane (DCM), ethanol, and dimethylformamide (DMF) were purchased from Tianjin Fuyu Fine Chemical (Tianjin, China). The melting points of target compounds were measured using a point apparatus (X-4, Beijing Taike Instrument Co., Ltd, Beijing, China) and were uncorrected. ^{1}H and ^{13}C NMR were collected using a spectrometer (AV-400, Bruker, Beijing, China) with tetramethylsilane as the internal standard. HRMS was obtained on a micrOTOF-Q II 10410 spectrometer (Bruker, Beijing, China) or a Waters Xevo G2-XS QTof spectrometer (Waters Technology, Shanghai, China). All solvents and reagents were of analytical reagent grade. The packing material used in the chromatographic column is a column chromatography silica gel with a mesh number between 100 and 200.

General Procedure for the Synthesis of Intermediate Compounds J2.1–9

A mixture of chlorobenzene (1 eq) J1.1–9, anhydrous K2CO3 (1.33 eq), phenol or thiophenol (1.3 eq), and CuCl (0.25 g) was stirred in DMF at 140 C for 10 h. The mixture was cooled to room temperature, then poured into 100 ml of water. The pH of the aqueous solution was adjusted to 2-4 with hydrochloric acid. The mixture was filtered off to give the desired solid products J2.1–9.

General Procedure for the Synthesis of Intermediate Compounds J3.1–9

Thionyl chloride (3 eq) and one drop of DMF in were added to a solution of J2.1–9 (1 eq) in DCM (40 ml). The mixture was stirred at 60 C for 1 h, then the solvent was removed under reduced pressure and afforded J3.1–9. The acyl chloride was used directly without further purification.

General Procedure for the Synthesis of Intermediate Compound J5

The 3,4,5,6-tetrahydrophthalic anhydride (J4) (1 eq) and urea (0.5 eq) were heated at 155 to 160 C until effervescence ceased and the mixture was almost completely solidified. The product was cooled and crystallized from the addition of ethanol to produce the white solid 3,4,5,6-tetrahydrophthalimide J5.

General Procedure for the Synthesis of Final Compound J6

The 4-dimethylaminopyridine (0.25 eq) was added to a stirred solution of 3,4,5,6-tetrahydrophthalimide (1 eq) J5, J3 (1.3 eq), and triethylamine (2 eq) in DCM (40 ml). The mixture was allowed to react at room temperature until the 3,4,5,6-tetrahydrophthalimide was completely consumed to yield J6 (as detected by thin-layer chromatography). The solvent was then removed in a vacuum, and the solid products were purified through chromatography on a silica gel using petroleum ether/ethyl acetate as eluent to produce the pure product.

https://doi.org/10.1017/wsc.2020.66 Published online by Cambridge University Press

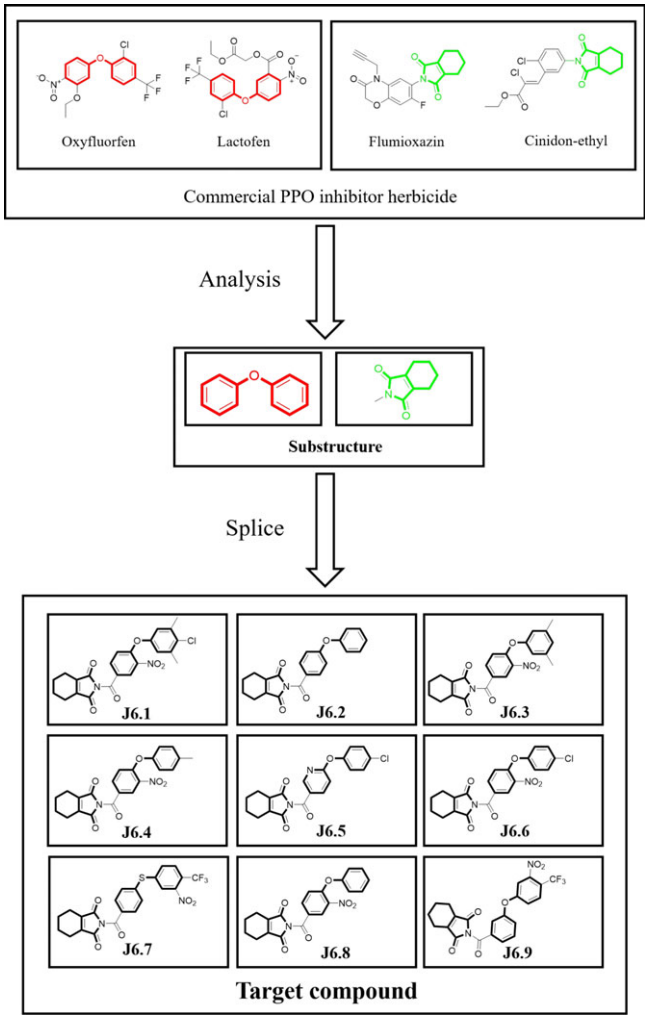


Figure 3. The design of the target compounds.

^{1}H NMR, ^{1}C NMR, and HRMS of Compounds J6.1–9

2-(4-(4-Chloro-3,5-Dimethylphenoxy)-3-Nitrobenzoyl)-4,5,6,7-Tetrahydro-1H-Isoindole-1,3(2H)-Dione (J6.1)

White solid. ^{1}H NMR (400 MHz, Chloroform-d) δ 8.33 (d, J = 2.3 Hz, 1H, Ar-H), 7.89 (dd, J = 8.9, 2.3 Hz, 1H, Ar-H), 6.97 (d, J = 8.8 Hz, 1H, Ar-H), 6.89 (s, 2H, Ar-H), 2.44 (h, J = 2.5, 2.1 Hz, 4H, $2CH_2$), 2.40 (s, 6H, $2CH_3$), 1.84 (p, J = 3.1 Hz, 4H, $2CH_2$). ^{13}C NMR (101 MHz, Chloroform-d) δ 167.65 (2), 163.63, 155.49, 151.50, 143.78 (2), 139.63, 138.74 (2), 135.69, 128.47, 131.85, 127.04, 120.20 (2), 118.17, 21.07 (2), 20.93 (2), 20.34 (2). Calculated for $C_{24}H_{24}ClN_2O_7$ $[M+CH3OH+H]^+$ 487.1272; found: 487.1270.

2-(4-Phenoxybenzoyl)-4,5,6,7-Tetrahydro-1H-Isoindole-1,3(2H)-Dione (J6.2)

White solid. ^{1}H NMR (400 MHz, Chloroform-d) δ 7.82-7.72 (m, 2H, Ar-H), 7.46-7.35 (m, 2H, Ar-H), 7.25-7.18 (m, 1H, Ar-H), 7.13-7.06 (m, 2H, Ar-H), 7.02-6.94 (m, 2H, Ar-H), 2.42 (h, J = 2.6, 2.1 Hz, 4H, $2CH_2$), 1.82 (p, J = 3.2 Hz, 4H, $2CH_2$). ^{13}C NMR (101 MHz, Chloroform-d) δ 168.22 (2), 165.40, 163.08, 155.00, 143.24 (2), 132.89 (2), 130.12 (2), 126.84, 124.96, 120.53 (2), 116.92 (2), 21.17 (2), 20.27 (2). Calculated for $C_{21}H_{18}NO_4$ $[M+H]^+$ 348.1236; found:348.1235.

2-(4-(3,5-Dimethylphenoxy)-3-Nitrobenzoyl)-4,5,6,7-Tetrahydro-1H-Isoindole-1,3(2H)-dione (J6.3)

White solid. ^{1}H NMR (400 MHz, Chloroform-d) δ 8.33 (d, J = 2.3 Hz, 1H, Ar-H), 7.88 (dd, J = 8.8, 2.2 Hz, 1H, Ar-H), 7.02-6.88 (m, 2H, Ar-H), 6.76 (d, J = 1.5 Hz, 2H, Ar-H), 2.44 (p, J = 2.9 Hz, 4H, $2CH_2$), 2.34 (s, 6H, $2CH_3$), 1.84 (p, J = 3.2 Hz, 4H, $2CH_2$). ^{13}C NMR (101 MHz, Chloroform-d) δ 167.69 (2), 163.73, 155.99, 153.73, 143.74 (2), 140.52 (2), 139.53, 135.63, 128.47, 127.75, 126.57, 118.14, 118.13 (2), 21.28 (2), 21.08 (2), 20.34 (2). Calculated for $C_{23}H_{21}N_2O_6$ $[M+H]^+$ 421.1400; found:421.1392.

2-(2-Nitro-4-(p-Tolyloxy)benzoyl)-4,5,6,7-Tetrahydro-1H-Isoindole-1,3(2H)-Dione (J6.4)

White solid. ^{1}H NMR (400 MHz, Chloroform-*d*) δ 8.33 (d, J = 2.2 Hz, 1H, Ar-H), 7.87 (dd, J = 8.8, 2.3 Hz, 1H, Ar-H), 7.24 (s, 1H, Ar-H), 7.06-7.00 (m, 2H, Ar-H), 6.94 (d, J = 8.9 Hz, 1H, Ar-H), 2.44 (p, J = 3.1 Hz, 4H, $2CH_2$), 2.39 (s, 3H, CH_3), 1.84 (p, J = 3.2 Hz, 4H, $2CH_2$). ^{13}C NMR (101 MHz, Chloroform-*d*) δ 167.67 (2), 163.70, 156.14, 151.50, 143.74 (2), 139.50, 135.98, 135.64, 130.95 (2), 128.52, 126.57, 120.48 (2), 117.78, 21.08, 20.88, 20.34. Calculated for $C_{22}H_{19}N_2O_6$ $[M+H]^+$ 407.1243; found:407.1235.

2-(6-(4-Chlorophenoxy)nicotinoyl)-4,5,6,7-Tetrahydro-1H-Isoindole-1,3(2H)-Dione (J6.5)

White solid. ^{1}H NMR (400 MHz, Chloroform-*d*) δ 8.52 (d, J = 2.4 Hz, 1H, pyridine-H), 8.10 (dd, J = 8.7, 2.4 Hz, 1H, pyridine-H), 7.46-7.33 (m, 2H, Ar-H), 7.18-7.07 (m, 2H, Ar-H), 7.00 (d, J = 8.7 Hz, 1H, pyridine-H), 2.42 (q, J = 3.0 Hz, 4H, 4H, $2CH_2$), 1.82 (p, J = 3.0 Hz, 4H, 4H, $2CH_2$). ^{13}C NMR (101 MHz, Chloroform-*d*) δ 167.76 (2), 166.38, 163.88, 151.46, 151.16, 143.55 (2), 141.30, 130.88, 129.80 (2), 124.15, 123.05 (2), 111.10, 21.10 (2), 20.29 (2). Calculated for $C_{21}H_{20}ClN_2O_5$ $[M+CH3OH+H]^+$ 415.1061; found: 415.1072.

2-(4-(4-Chlorophenoxy)-3-Nitrobenzoyl)-4,5,6,7-Tetrahydro-1H-Isoindole-1,3(2H)-Dione (J6.6)

White solid. ^{1}H NMR (400 MHz, Chloroform-*d*) δ 8.34 (d, J = 2.2 Hz, 1H, Ar-H), 7.90 (dd, J = 8.8, 2.3 Hz, 1H, Ar-H), 7.47-7.39 (m, 2H, Ar-H), 7.13-7.05 (m, 2H, Ar-H), 6.97 (d, J = 8.8 Hz, 1H, Ar-H), 2.44 (p, J = 3.0 Hz, 4H, $2CH_2$), 1.84 (p, J = 3.2 Hz, 4H, $2CH_2$).^{13}C NMR (101 MHz, Chloroform-*d*) δ 167.60 (2), 163.54, 155.04, 152.58, 143.83 (2), 139.88, 135.72, 131.43, 130.56 (2), 128.51, 127.52, 121.77 (2), 118.28, 21.06, 20.35. Calculated for $C_{21}H_{15}ClN_2NaO_6$ $[M+Na]^+$ 449.0516; found: 449.0513.

2-(4-((3-Nitro-4-(Trifluoromethyl)phenyl)thio)benzoyl)-4,5,6,7-Tetrahydro-1H-Isoindole-1,3(2H)-Dione (J6.7)

White solid. ^{1}H NMR (400 MHz, Chloroform-*d*) δ 8.52 (dd, J = 1.9, 0.9 Hz, 1H), 7.90-7.84 (m, 2H), 7.71-7.65 (m, 2H), 7.63-7.57 (m, 1H), 7.05 (d, J = 8.6 Hz, 1H), 2.45 (p, J = 3.2 Hz, 4H), 1.84 (p, J = 3.2 Hz, 4H).^{13}C NMR (101 MHz, Chloroform-*d*) δ 167.66 (2), 165.39, 144.83, 143.66 (2), 142.60, 136.72, 135.26 (2), 134.76, 131.60 (2), 129.79, 129.33 (2), 123.25 (2), 21.10 (2), 20.32 (2). Calculated for $C_{22}H_{16}F_3N_2O_5S$ $[M+H]^+$ 477.0732; found: 477.0721.

2-(3-Nitro-4-phenoxybenzoyl)-4,5,6,7-Tetrahydro-1H-Isoindole-1,3(2H)-Dione (J6.8)

White solid. ^{1}H NMR (400 MHz, Chloroform-*d*) δ 8.35 (d, J = 2.2 Hz, 1H, Ar-H), 7.88 (dd, J = 8.9, 2.3 Hz, 1H, Ar-H), 7.51-7.42 (m, 2H, Ar-H), 7.35-7.27 (m, 1H, Ar-H), 7.20-7.10 (m, 2H, Ar-H), 6.96 (d, J = 8.9 Hz, 1H, Ar-H), 2.44 (p, J = 3.2 Hz, 4H, $2CH_2$), 1.84

https://doi.org/10.1017/wsc.2020.66 Published online by Cambridge University Press

(p, $J = 3.2$ Hz, 4H, $2CH_2$).^{13}C NMR (101 MHz, Chloroform-*d*) δ 167.64 (2), 155.68, 153.87, 143.76 (2), 139.68, 135.66, 130.49 (2), 128.51, 126.90, 126.09, 120.58 (2), 118.11, 21.06 (2), 20.33 (2). Calculated for $C_{22}H_{21}N_2O_7$ $[M+CH3OH+H]^+$ 425.1349; found: 425.1341.

2-(3-(3-Nitro-4-(Trifluoromethyl)phenoxy)benzoyl)-4,5,6,7-Tetrahydro-1H-Isoindole-1,3(2H)-Dione (J6.9)

White solid. ^{1}H NMR (400 MHz, Chloroform-*d*) δ 8.24 (d, $J = 2.2$ Hz, 1H Ar-H), 7.76 (dd, $J = 8.9$, 2.3 Hz, 1H Ar-H), 7.70 (dt, $J = 7.8$, 1.3 Hz, 1H Ar-H), 7.57 (t, $J = 7.9$ Hz, 1H Ar-H), 7.49-7.44 (m, 1H Ar-H), 7.38 (ddd, $J = 8.2$, 2.5, 1.0 Hz, 1H Ar-H), 7.11 (d, $J = 8.8$ Hz, 1H Ar-H), 2.41 (h, $J = 2.6$ Hz, 4H, $2CH_2$), 1.82 (p, $J = 3.1$ Hz, 4H, $2CH_2$). ^{13}C NMR (101 MHz, Chloroform-*d*) δ 167.64 (2), 165.07, 154.17, 153.13, 143.59 (2), 140.42, 135.36, 131.02, 130.98, 130.62, 127.38, 125.44, 123.64, 123.60, 121.60, 119.76, 21.06 (2), 20.27 (2). Calculated for $C_{22}H_{16}F_3N_2O_6$ $[M+H]^+$ 461.0960; found: 461.0598.

In Vitro Inhibition Experiments of Maize PPO

The preparation of maize PPO was carried out using a previously reported method (Li et al. 2007). The enzyme catalytic rate was calculated by measuring the amount of protoporphyrin IX produced by the enzyme product over a period of time. The concentration of protoporphyrin IX could be determined by the absorbance monitored by a multifunctional microplate reader (TECAN [Shanghai] Trading Co., Ltd., Shanghai China) at a wavelength of 410 nm (Jiang et al. 2011). Before use, the compounds J6.1–9 were dissolved in acetonitrile and diluted with buffer to achieve compounds with different concentrations. The formula used in the calculation of inhibition rate is as follows:

$$I = \frac{X - Y}{X} \times 100\% \quad [1]$$

where I is the inhibition rate, X is the catalytic rate of the blank group, and Y is the catalytic rate of compound with certain concentration. The IC_{50} value was obtained by SPSS 20.0 (Chicago, Illinois) analysis of the inhibitory rates of the compounds obtained at various concentrations. Oxyfluorfen and flumioxazin were used as positive controls, and each experiment was repeated three times.

Herbicidal Activity

The herbicidal activity of compounds J6.1–9 on three representative monocotyledon weeds, green foxtail [*Setaria viridis* (L.) Beauv.] (SETVP), annual bluegrass (*Poa annua* L.) (POAAN), and barnyardgrass [*Echinochloa crus-galli* (L.) Beauv.] (ECHCG), and three representative dicotyledon weeds, velvetleaf (*Abutilon theophrasti* Medik.) (ABUTH), shepherd's purse [*Capsella bursa-pastoris* (L.) Medik.] (CAPBP), and common purslane (*Portulaca oleracea* L.) (POROL), was tested according to a previously reported method (Fu et al. 2019a, 2019b). Before the test, the compounds J6.1–9 were was prepared as an emulsion. In a typical preparation, 10 mg of the compound was precisely weighed and then dissolved in 2 ml of acetonitrile. After this, an appropriate amount of emulsifiable concentrate was added as an emulsifier, and acetonitrile was then added to make up to 10 ml. If necessary, a pipette was used to dispense an appropriate amount of this solution, and the solution was diluted to the required concentration. Plastic pots (8-cm diameter) were filled with clay to a depth of 8 to 10 cm, and 10 to 30 seeds of the same variety were planted in individual pots and covered with 1 to 3 cm of soil During weed growth, the room temperature was maintained at 15 to 30 C, and the relative humidity was maintained at 50%. Single-leaf weeds in the 1-leaf stage and dicotyledonous weeds in the 2-leaf stage were treated with the series of diluted J6 emulsions. Compound emulsions were sprayed on plants from a height of 10 cm. The dosage of the spray was between 37.5 and 150 g ai ha^{-1}, and the spray dose was calculated by dividing the mass of the sprayed compound by the area exposed to the spray. The common commercial herbicides oxyfluorfen (Yifan Biological Technology Group Co., Ltd., Wenzhou, China), and flumioxazin (Sichuan Lier Crop Science Co., Ltd. Chengdu, China) were used as controls. Oxyfluorfen was in the form of 24% emulsifiable concentrate, while flumioxazin was in the form of 50% wettable powder. The herbicidal activity was visually observed within 15 to 30 d after the treatment. Each experiment was repeated three times.

Crop Tolerance

Three representative crops (peanut, cotton, and maize) were selected to assess the greenhouse crop tolerance for J6.3. Seeds for each crop were sown in individual pots (8-cm diameter) and grown under the following conditions: room temperature maintained at 15 to 30 C and relative humidity maintained at 50% After the crop reached the 4-leaf stage, it was treated with a dose of 75 to 300 g ai ha^{-1} of J6.3. The crop tolerance of J6.3 for the crops was visually observed (the injured volume of the plant) within 7 to 10 d after spraying. Oxyfluorfen and flumioxazin were used as positive controls. Each experiment was repeated three times.

Herbicidal Activity against Resistant Weeds

Due to the long-term and widespread use of PPO inhibitors, it is necessary to develop new herbicides to control the PPO-resistant weeds. To investigate whether J6.3 could effectively control PPO-resistant weeds, its herbicidal activity was investigated on some of representative PPO-resistant weeds (data from http://weedscience.org/Pages/MOA.aspx?MOAID=8) such as common ragweed (*Ambrosia artemisiifolia* L.) (AMBEL), weed resistant to oxyfluorfen and flumioxazin), rigid ryegrass (*Lolium rigidum* Gaudin) (LOLRI) (LR, weed resistant to oxyfluorfen), Asian copperleaf (*Acalypha australis* L.) (ACAAU), weed resistant to fomesafen), and flixweed [*Descurainia sophia* (L.) Webb ex Prantl] (DESSO, weed resistant to carfentrazone-ethyl), according to the method outlined in "Herbicidal Activity."

Molecular Docking Experiment

During the molecular docking experiment, tobacco (*Nicotiana tabacum* L.) PPO was selected as the docking enzyme. The crystal data for this enzyme were downloaded from the RCSB Protein Database (https://www.rcsb.org/structure/1sez) (PDB ID:1SEZ) The 3D structures of J6.1–9 were constructed using SYBYL 6.9 (Tripos, St Louis, MO, USA). The charges of all compounds were calculated using the Gasteiger-Huckel method, and the structures of J6.1–9 were optimized. Discovery Studio 3.5 (BIOVIA Inc., San Diego, USA) was used to calculate the interaction between two molecules, with a total of 258 runs per molecule. The optimal binding mode was selected by comparing the eutectic ligands in mitchondrial PPO (Ye et al. 2018; Zhang et al. 2020b).

https://doi.org/10.1017/wsc.2020.66 Published online by Cambridge University Press

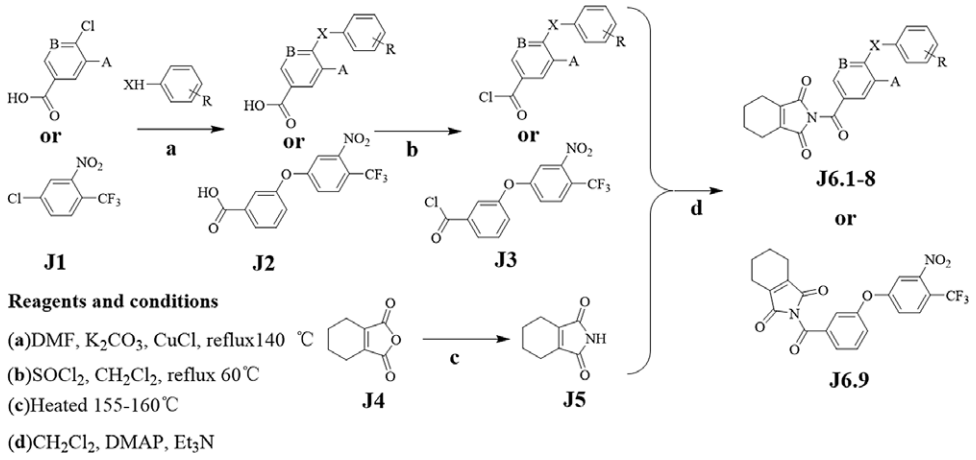


Figure 4. Synthesis of diphenyl ether derivative containing tetrahydrophthalimide J6.1–9.

Results and Discussion

Results and Discussion of Synthesis

The synthesis of J6.1–9 is shown in Figure 4. Intermediate J2 was prepared by a modified Williamson synthesis method (Hossian and Jana 2016; Li and Zhang 2013; Matsuo et al. 1985). Potassium carbonate was selected as the neutralizing reagent, CuCl was selected as the catalyst, and DMF was selected as the solvent. J1 and different types of phenols were used as the raw materials in the preparation of intermediate J2. Subsequently, J2 was reacted with thionyl chloride in DCM to obtain the active intermediate J3 (Jones et al. 2018; Urai et al. 2017). J3 could be reacted directly with compound J5 without purification to obtain the final product J6 (Cui et al. 2017; Meng and Szostak 2016; Wang et al. 2014). Diphenyl ether structure with carboxyl group J2 is an important intermediate for the synthesis of the final product. Hydroxybenzoic acid was initially selected to react with chlorobenzene to obtain intermediate J2. Unfortunately, the total yield of the final product J6.9 was only at 28%. The low total yield of the final product J6.9 can presumably be attributed to the strong electron-withdrawing properties of the carboxyl group, which reduces the nucleophilicity of phenol. The low nucleophilicity of phenol reduced the yield of intermediate J2 (Begunov et al. 2015).

Thus, the synthesis strategy was improved in subsequent experiments. Finally, the use of chlorobenzoic acid and different types of phenols with electron-donating groups as raw materials in the preparation of intermediate J2 greatly improved the yield. In addition, the choice of neutralizing reagent could greatly affect the yield of the acylation reaction. Potassium carbonate was initially selected as the acid for the acylation reaction, but the yields were unsatisfactory. Fortunately, replacing K_2CO_3 with Et_3N as the neutralizing reagent led to improved yield. All synthesized final products J6.1–9 (Table 1) were purified by column chromatography, and their structures were characterized by melting point (mp),^{1}H NMR, ^{13}C NMR, and HRMS. For detailed NMR and HRMS data, please refer to the Supplementary Material.

PPO Inhibition Activity and SAR

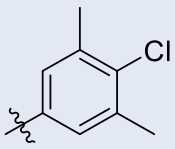
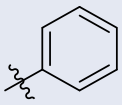
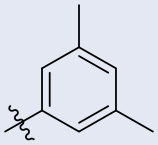
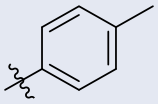
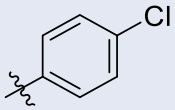
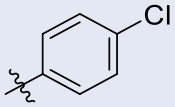
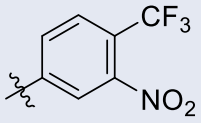
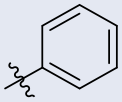
As shown in Table 2, the newly synthesized compounds show potential enzyme inhibitory activity against maize PPO, with IC_{50} values ranging from 4.7 to 5,531.1 nM. Among them, J6.1 and J6.3 show enhanced enzyme inhibitory activity compared with the commercial herbicide oxyfluorfen and flumioxazin. J6.3 exhibits the highest enzyme inhibitory activity among all newly synthesized compounds, with an IC_{50} value of 4.7 nM. The potency of this PPO inhibitor in vitro is 25 times higher than that of oxyfluorfen (IC_{50} = 117.9 nM), and it is also 33 times higher than that of flumioxazin (IC_{50} = 157.1 nM). Based on Table 2, it is shown that J6.1, J6.3, and J6.4 show excellent activity. All these samples have a common feature in which their R substituents contain methyl groups. Correspondingly, the activity of J6.4 is significantly reduced after replacing the methyl group with chlorine (J6.6). Thus, the introduction of methyl group into the R group of the compound can enhance its activity. In addition, the activities of J6.2 and J6.8 are also significantly different. The only structural difference between J6.2 and J6.8 is the difference in the A substituents, whereby one is hydrogen while the other is a nitro group. When the A substituent is a nitro group, the enzyme inhibitory activity of the compound is enhanced. In addition, when the diphenyl ether structure of J6.9 is replaced with diphenyl sulfide (to achieve J6.7), the enzyme inhibitory activity of J6.9 is significantly reduced. In short, retaining the diphenyl ether structure of the compound, introducing a methyl group into the R substituent, and changing the A substituent to a nitro group are beneficial for enhancing the enzyme inhibitory activity of the compound.

Herbicidal Activity and Crop Tolerance

Table 2 shows the POST herbicidal results of J6.1–9 on three representative monocotyledonous weeds; *S. viridis*, *P. annua*, and *E. crus-galli*, and three representative dicotyledonous weeds *A. theophrasti*, *C. bursa-pastoris*, and *P. oleracea*. At 1 to 2 d after spraying with J6.1–9, the leaves of some weeds exhibited loose, wet foliage. They may also show burn symptoms, which are later bleached and subsequently wilted. This result suggests that these synthetic compounds may be PPO inhibitors. As shown in Table 2, most compounds show a certain herbicidal activity at a dose of 150 g ai ha^{-1}, in particular for *A. theophrasti*. Furthermore, J6.1, J6.3, J6.4, J6.5, J6.6, and J6.8 show strong inhibitory activity (inhibition rate ≥80%) against *A. theophrasti*, and they were therefore selected for further screening. When the dose is reduced to 75 g ai ha^{-1}, the inhibitory activity of J6.4, J6.5, and J6.8 are significantly reduced. J6.1 and J6.3 show excellent herbicidal activity even at doses as low as 37.5 g ai ha^{-1}. However, only J6.3 is able to demonstrate broad-spectrum herbicidal properties. The inhibitory activities of J6.3 on

https://doi.org/10.1017/wsc.2020.66 Published online by Cambridge University Press

Table 1. The structures and the physicochemical properties of compounds J6.1–9.[a]

Compound	R	X	A	B	Yield	mp
					—%—	C
J6.1		O	NO_2	C	81	194.6–195.1
J6.2		O	H	C	78	154.1–154.8
J6.3		O	NO_2	C	87	156.7–156.8
J6.4		O	NO_2	C	80	193.9–194.0
J6.5		O	H	N	48	165.2–165.9
J6.6		O	NO_2	C	80	201.9–202.6
J6.7		S	H	C	37	143.6–144.5
J6.8		O	NO_2	C	59	127.2–127.9
J6.9	—	—	—	—	28	103.3–105.5

[a]Generic structure of compound J6.1–9 is shown in Figure 4.

the six selected weeds are comparable to those of oxyfluorfen. In addition, the inhibitory activity of J6.3 on monocotyledonous weeds is significantly greater than that of flumioxazin. Furthermore, the herbicidal activity of the compound is consistent with the enzyme inhibitory activity. For instance, J6.1, J6.3, and J6.4 exhibit high herbicidal activity, and all these compounds have a methyl group as the R substituent. The herbicidal activity of J8 with a nitro group as A substituent is obviously greater than that of J2 without a nitro group as A substituent. In view of the excellent herbicidal activity of J6.3, we also tested its crop tolerance. As shown in Table 3, even at a dose of 300 g ai ha^{-1}, cotton and peanut still show tolerance (injury rate ≤10%) to J6.3. However, at a dose of 300 g ai ha^{-1}, oxyfluorfen exhibits no safety for peanut and cotton. Although J6.3 is not as safe as flumioxazin when applied to the crops, the herbicidal activity of J6.3 is significantly higher than that of flumioxazin. In summary, J6.3 can be further developed as a potential herbicide candidate for peanut and cotton fields.

Herbicidal Activity against Resistant Weeds

To verify whether J6.3, with its excellent herbicidal activity, can control PPO-resistant weeds, some representative PPO-resistant weeds were selected for this work. As shown in Table 4, among the four PPO-resistant weeds, J6.3 can effectively control *L. rigidum*, *A. australis*, and *D. sophia*. The failure of J6.3 in controlling *A. artemisiifolia* could be due to the fact that *A. artemisiifolia* is resistant to both diphenyl ether and *N*-phenylphthalimide herbicides. Fortunately, J6.3 can effectively control *L. rigidum* and *A. australis*, which oxyfluorfen is unable to control. This could be due to the presence of flumioxazin as an active ingredient in J6.3, as flumioxazin has been shown to effectively control *L. rigidum* and *A. australis* in Table 4. By extension, J6.3 is able to control *L. rigidum* and *A. australis*, as observed in the "Results." Therefore, introducing a diphenyl ether structure and a tetrahydrophthalimide structure in J6.3 may lead to the synergistic

https://doi.org/10.1017/wsc.2020.66 Published online by Cambridge University Press

Table 2. Herbicidal activity and maize protoporphyrinogen oxidase inhibitory activities of compounds J6.1–9.[a]

Compound	Dose[b]	ABUTH	CAPBP	POROL	SETVP	POAAN	ECHCG	IC_{50}[c]
	—g ai ha^{-1}—							—nM—
J6.1	150	++++	++	++++	++++	+++	+++	30.0 ± 1.3 a
	75	+++	+	+++	+++	++	+++	
	37.5	++	–	++	+++	++	+++	
J6.2	150	+	–	–	–	–	–	3,383.3 ± 336.3 c
J6.3	150	++++	++++	++++	++++	++++	++++	4.7 ± 0.4 a
	75	++++	+++	++++	++++	++++	++++	
	37.5	++++	+++	++++	++++	+++	++++	
J6.4	150	+++	+++	++	++	+	+++	156.7 ± 7.9 a
	75	++	+	–	–	–	++	
J6.5	150	+++	–	–	–	–	–	1,285.6 ± 32.9 b
	75	+	–	–	–	–	–	
J6.6	150	++++	++	++	–	–	+	1,434.2 ± 1 03.1 b
	75	+++	+	–	–	–	–	
	37.5	++	–	–	–	–	–	
J6.7	150	–	–	–	–	–	–	5,331.1 ± 123.3 e
J6.8	150	+++	++	+	++	+	+	224.3 ± 13.5 a
	75	++	+	–	+	–	–	
J6.9	150	–	–	–	–	–	–	5,014.9 ± 134.9 d
Oxyfluorfen	150	++++	++++	+++	++++	++++	++++	117.9 ± 10.5 a
	75	++++	+++	+++	++++	++++	++++	
	37.5	++++	+++	+++	++++	++++	++++	
Flumioxazin	150	++++	++++	++++	+++	++	+++	157.1 ± 11.4 a
	75	++++	++++	++++	+	+	++	
	37.5	++++	+++	++++	+	+	++	

[a] Abbreviations and symbols: Three representative dicotyledonous weeds: green foxtail [*Setaria viridis (L.) Beauv.*] (SETVP), annual bluegrass (*Poa annua L.*) (POAAN), and barnyardgrass [*Echinochloa crus-galli (L.) Beauv.*] (ECHCG), and three representative dicotyledon weeds, velvetleaf (*Abutilon theophrasti Medik.*) (ABUTH), shepherd's purse [*Capsella bursa-pastoris (L.) Medik.*] (CAPBP), and common purslane (*Portulaca oleracea L.*) (POROL). Evaluation index of herbicidal activity (percentage of inhibition): ++++, ≥ 90%; +++, 80%–89%; ++, 60%–79%; +, 50%–59%; –, <50%.
[b] Compound emulsions were sprayed on plants from a height of 10 cm.
[c] Different letters indicate significant differences in values in the same column ($P < 0.05$).

Table 3. Greenhouse crop tolerance of compound J6.3.[a]

		Injury rating		
Compound	Dose	Peanut	Cotton	Maize
	—g ai ha^{-1}—		—%—	
J6.3	150	0	0	10
	300	0	10	30
Oxyfluorfen	150	10	20	5
	300	30	50	10
Flumioxazin	150	0	0	0
	300	0	0	5

[a] After the crop reached the 4-leaf stage, it was treated with a dose of 75–300 g ai ha^{-1} of J6.3. Compound emulsions were sprayed on plants from a height of 10 cm. The crop tolerance of J6.3 for the crops was visually observed (the injured volume of the plant) within 7–10 d after spraying. Oxyfluorfen and flumioxazin were used as positive controls.

Table 4. Inhibitory activity of J6.3 against resistant weeds.[a]

Compound	Dose[b]	AMBEL	LOLRI	ACAAU	DESSO
	—g ai ha^{-1}—				
J6.3	150	++	++++	++++	++++
	75	–	+++	++++	++++
	37.5	–	+++	+++	++++
Oxyfluorfen	150	–	++	+++	++++
	75	–	+	++	++++
	37.5	–	–	+	++++
Flumioxazin	150	+++	+++	++++	++++
	75	+	++	++++	++++
	37.5	–	++	++++	++++

[a] Abbreviations and symbols: common ragweed (*Ambrosia artemisiifolia L.*) (AMBEL), rigid ryegrass (*Lolium rigidum Gaudin*) (LOLRI), Asian copperleaf (*Acalypha australis L.*) (ACAAU), and flixweed [*Descurainia sophia (L.) Webb ex Prantl*] (DESSO). Evaluation index of herbicidal activity (percentage of inhibition): ++++, ≥90%; +++, 80%–89%; ++, 60%–79%; +, 50%–59%; –, <50%.
[b] Compound emulsions were sprayed on plants from a height of 10 cm.

https://doi.org/10.1017/wsc.2020.66 Published online by Cambridge University Press

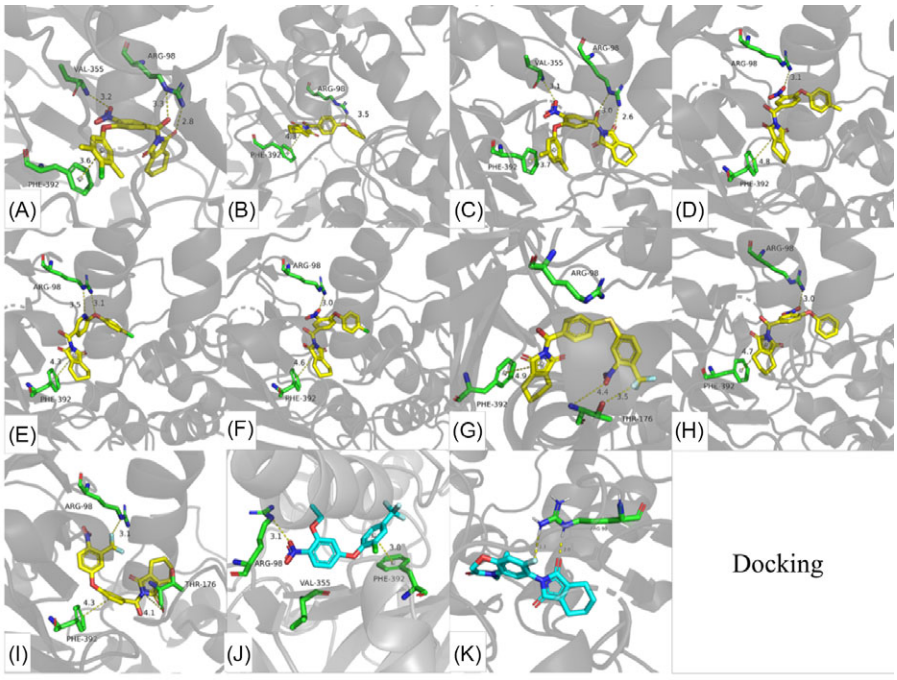


Figure 5. Docking modeling of compounds J6.1 (A), J6.2 (B), J6.3 (C), J6.4 (D), J6.5 (E), J6.6 (F), J6.7 (G), J6.8 (H), J6.9 (I), oxyfluorfen (J), and flumioxazin (K) to protoporphyrinogen oxidase in the active site. Yellow line represents carbon atoms, light yellow line represents sulfur atoms, red line represents oxygen atoms, light blue line represents nitrogen atoms, and green line represents chlorine atoms. Yellow dotted lines represent molecular forces.

combination of the activities of diphenyl ether herbicide and *N*-phenylphthalimide herbicide. Hence, J6.3 is unable to control *A. artemisiifolia* due to the resistance of *A. artemisiifolia* to both diphenyl ether herbicide and *N*-phenylphthalimide herbicide. On the other hand, J6.3 is able to control *D. sophia*, as *D. sophia* possesses resistance only to *N*-phenyl-triazolinone herbicide, but not to diphenyl ether herbicide and *N*-phenylphthalimide herbicide.

Results and Discussion of Docking

To study the mechanism of action of J6.1–9 and to explain the SAR, docking studies were performed on J6.1–9. The commercial herbicides oxyfluorfen and flumioxazin, were used as controls. As shown in Figure 5J, a benzene ring of oxyfluorfen forms a π–π stacking interaction with the amino acid residue Phe-392, while the nitro group of oxyfluorfen forms a hydrogen bond with the amino acid residue Arg-98. As shown in Figure 5K, flumioxazin forms two hydrogen bonds with amino acid residue Arg-98. The amino acid residue Arg-98 participates in the localization of the tetrapyrrole ring during the catalytic process of protoporphyrinogen IX (Dayan et al. 2018; Zhao et al. 2020). As shown in Figure 5, all the newly synthesized compounds, other than compound J6.7, share a common feature with oxyfluorfen. It is shown that all these compounds form hydrogen bonds with amino acid residue Arg-98, and they also form π–π stacking interaction with amino acid residue Phe-392. However, J6.7 is only able to form hydrogen bonds with amino acid residue Thr-176, which is not important for the enzymatic process. This may be the reason behind the significantly lower activity exhibited by J6.7 compared with the other newly synthesized compounds. From Figure 5A and C, it can be observed that the tetrahydrophthalimide structures of J6.1 and J6.3 form two hydrogen bonds with the amino acid residue Arg-98, and the nitro groups of J6.1 and J6.3 form a hydrogen bond with amino acid residue Val-355. However, oxyfluorfen only forms a hydrogen bond with amino acid residue Arg-98, and it does not form a hydrogen bond with amino acid residue Val-355. In addition, flumioxazin only forms hydrogen bonds with amino acid residues in the catalytic region, and it does not form π–π stacking interaction. This indicates that J6.1 and J6.3 bind more tightly to the amino acid residues of PPO compared with both oxyfluorfen and flumioxazin. As such, this may result in the higher enzyme inhibitory activities exhibited by J6.1 and J6.3 compared with oxyfluorfen and flumioxazin.

It can be observed in Figure 5 that the compounds other than J6.1 and J6.3 possess a tetrahydrophthalimide structure, which forms a π–π stacking interaction with the amino acid residue Phe-392. Furthermore, the distance between the tetrahydrophthalimide and the amino acid residue Phe-392 is longer compared with the distance between the benzene ring and the amino acid residue Phe-392. As a result, the π–π stacking interaction formed between the benzene ring and the amino acid residue Phe-392 is stronger than the π–π stacking interaction formed between tetrahydrophthalimide and the amino acid residue Phe-392. Interestingly, the R substituents of J6.1 and J6.3 have substituents at the 3 and 5 positions, while the R substituents of other compounds do not have substituents at the 3 and 5 positions. Thus, the activity of the compound can be enhanced by introducing groups at the 3 and 5 positions of the R substituent of the compound.

In addition, it was found that the introduction of a nitro group can enhance the activity of the compound. When amino acid residue Arg-98 is combined with other structures, a nitro group can form a hydrogen bond with amino acid residue Val-355 (J6.1 and J6.3). When the amino acid residue Arg-98 forms a hydrogen bond with the nitro group (J6.4, J6.6, J6.8, and J6.9), the length of its hydrogen bond is shorter than the hydrogen bond formed between

https://doi.org/10.1017/wsc.2020.66 Published online by Cambridge University Press

the phenoxy group structure and the amino acid residue Arg-98 (J6.2 and J6.5). In short, the introduction of nitro group can enhance the intermolecular forces between the compound and the amino acid in the catalytic region of PPO so as to improve the activity of the compound.

In conclusion, in order to find new PPO inhibitors with higher biological activity, a series of diphenyl ether derivatives containing tetrahydrophthalimide structure were designed and synthesized in this work. Several compounds with relatively low IC_{50} values were found. Among these compounds, J6.3, 2-(4-(3,5-dimethylphenoxy)-3-nitrobenzoyl)-4,5,6,7-tetrahydro-1H-isoindole-1,3(2H)-dione, with a IC_{50} value of 4.7 nM, is able to a demonstrate 25-fold increase in activity compared with oxyfluorfen (IC_{50} = 117.9 nM), and a 33-fold increase in activity compared with flumioxazin (IC_{50} = 157.1 nM) against maize PPO. As such, based on these results, J6.3 is the most potent compound among the compounds synthesized. In POST application, J6.3 shows excellent herbicidal activity at a dose of 37.5 g ai ha^{-1}, which is comparable to that of oxyfluorfen, and this result is greater than that of flumioxazin. Even at a dose of 300 g ai ha^{-1}, peanut and cotton are still able to demonstrate greater tolerance to J6.3. Experiments on the herbicidal activity of resistant weeds reveal that the introduction of diphenyl ether structure and tetrahydrophthalimide structure in J6.3 presumably leads to the synergistic combination of the activities of the diphenyl ether herbicide and *N*-phenylphthalimide herbicide. Therefore, J6.3 could be developed as a new herbicide candidate for cotton and peanut fields. In addition, the PPO enzyme inhibitory activity experiments, greenhouse herbicidal activity experiments, molecular docking, and herbicidal activity against resistant weeds experiments provide direction for further structural optimization. Three main conclusions can be made based on the results: First, the splicing of diphenyl ether and *N*-phenylphthalimide can combine the activities of two types of herbicides. Second, the introduction of a nitro group can help the compound to form more stable hydrogen bonds with surrounding amino acid residues. Finally, the introduction of substituents at the 3 and 5 positions of the R substituent is beneficial, as these substituents can form π–π stacking interactions with the surrounding amino acid residues.

Acknowledgments. The authors are grateful to Jia-Zhong Li (Lanzhou University) for assistance with molecular docking analyses and Chun-Hong Teng (Agronomy College, Northeast Agricultural University) for assistance with the bioactivity assay. This research was supported by the National Natural Science Foundation of China (31572042), the Natural Science Foundation of Heilongjiang Province (ZD2017002), the Heilongjiang Province Postdoctoral Research Startup Fund (LBH-Q19083), and the Research Science Foundation in Technology Innovation of Harbin (2017RAQXJ017). The authors have declared no conflicts of interest.

Supplementary material. To view supplementary material for this article, please visit https://doi.org/10.1017/wsc.2020.66

References

Alcantara-de la Cruz R, Dominguez-Martinez PA, Silveira HM, Cruz-Hipolito HE, Palma-Bautista C, Vazquez-Garcia JG, Dominguez-Valenzuela JA, De Prado R (2019) Management of glyphosate-resistant weeds in Mexican citrus groves: chemical alternatives and economic viability. Plants 8:325

Begunov RS, Valyaeva AN, Belyaev VV, Dobretsova NO (2015) Ultrasound synthesis of diaryl ethers. Russ Chem Bull 64:1971–1974

Cui M, Chen Z, Liu T, Wang H, Zeng Z (2017) N-acylsuccinimides: efficient acylative coupling reagents in palladium-catalyzed Suzuki coupling via CN cleavage. Tetrahedron Lett 58:3819–3822

Dayan FE, Barker A, Tranel PJ (2018) Origins and structure of chloroplastic and mitochondrial plant protoporphyrinogen oxidases: implications for the evolution of herbicide resistance. Pest Manag Sci 74:2226–2234

Dayan FE, Dayan EA (2011) Porphyrins: one ring in the colors of life a class of pigment molecules binds King George III, vampires and herbicides. Am Sci 99:236–243

Duke SO, Lydon J, Becerril JM, Sherman TD, Lehnen LP, Matsumoto H (1991) Protoporphyrinogen oxidase-inhibiting herbicides. Weed Sci 39:465–473

Fu Y, Zhang SQ, Liu YX, Wang JY, Gao S, Zhao LX, Ye F (2019a) Design, synthesis, SAR and molecular docking of novel green niacin-triketone HPPD inhibitor. Ind Crop Prod 137:566–575

Fu Y, Zhang D, Zhang S, Liu Y, Guo Y, Wang M, Gao S, Zhao L-X, Ye F (2019b) Discovery of N-aroyl diketone/triketone derivatives as novel 4-hydroxyphenylpyruvatedioxygenase inhibiting-based herbicides. J Agric Food Chem 67:11839–11847

Gao S, Liu YY, Jiang JY, Li XM, Zhao LX, Fu Y and Ye F (2020) Encapsulation of thiabendazole in hydroxypropyl-β-cyclodextrin nanofibers via polymer-free electrospinning and its characterization. Pest Manag Sci, 10.1002/ps.5885

Heap I, Duke SO (2018) Overview of glyphosate-resistant weeds worldwide. Pest Manag Sci 74:1040–1049

Hossian A, Jana R (2016) Carboxyl radical-assisted 1,5-aryl migration through Smiles rearrangement. Org Biomol Chem 14:9768–9779

Jiang LL, Zuo Y, Wang ZF, Tan Y, Wu QY, Xi Z, Yang GF (2011) Design and syntheses of novel N-(benzothiazol-5-yl)-4,5,6,7-tetrahydro-1H-isoindole-1,3(2H)-dione and N-(benzothiazol-5-yl)isoindoline-1,3-dione as potent protoporphyrinogen oxidase inhibitors. J Agric Food Chem 59:6172–6179

Jones JW, Price TL, Huang FH, Zakharov L, Rheingold AL, Slebodnick C, Gibson HW (2018) Pseudocryptand hosts for paraquats and diquats. J Org Chem 83:823–834

Kaur S, Sandell LD, Lindquist JL, Jhala AJ (2014) Glyphosate-resistant giant ragweed *(Ambrosia trifida)* control in glufosinate-resistant soybean. Weed Technol 28:569–577

Li AJ, Zhang HX (2013) Synthesis of diflufenican. Agrochem 52:565–567

Li HB, Li YH, Liu B, Wang YF, Wu C, Zou XM, Yang HZ (2007) Study of method for measuring the inhibition of protoporphyrinogen oxidase activity in vitro. J Plant Physiol 43:1152–1156

Matsuo M, Taniguchi K, Katsura Y, Kamitani T, Ueda I (1985) New 2-aryliminoimidazolidines. 1. Synthesis and antihypertensive properties of 2-(2-phenoxyphenylimino)imidazolidines and related-compounds. Chem Pharm Bull 33:4409–4421

Meng GR, Szostak M (2016) Rhodium-catalyzed C-H bond functionalization with amides by double C-H/C-N bond activation. Org Lett 18:796–799

Powles SB (2008) Evolved glyphosate-resistant weeds around the world: lessons to be learnt. Pest Manag Sci 64:360–365

Qin XH, Sun L, Wen X, Yang X, Tan Y, Jin H, Cao QY, Zhou WH, Xi Z, Shen YQ (2010) Structural insight into unique properties of protoporphyrinogen oxidase from *Bacillus subtilis*. J Struct Biol 170:76–82

Schryver MG, Soltani N, Hooker DC, Robinson DE, Tranel PJ, Sikkema PH (2017) Control of glyphosate-resistant common waterhemp *(Amaranthus rudis)* in three new herbicide-resistant soybean varieties in ontario. Weed Technol 31:828–837

Shibata A, Kodaka R, Fujisawa T, Katagi T (2011) Degradation of flumioxazin in illuminated water-sediment systems. J Agric Food Chem 59:11186–11195

Ucles S, Hakme E, Ferrer C, Fernandez-Alba AR (2018) Analysis of thermally labile pesticides by on-column injection gas chromatography in fruit and vegetables. Anal Bioanal Chem 410:6861–6871

Urai Á, Váradi A, Szőcs L, Komjáti B, Le Rouzic V, Hunkele A, Pasternak GW, Majumdar S, Hosztafi S (2017) Synthesis and pharmacological evaluation of novel selective MOR agonist 6β-pyridinyl amidomorphines exhibiting long-lasting antinociception. Med Chem Commun 8:152–157

Wang BF, Wen X, Qin XH, Wang ZF, Tan Y, Shen YQ, Xi Z (2013) Quantitative structural insight into human variegate porphyria disease. J Biol Chem 288:11731–11740

Wang DW, Li Q, Wen K, Ismail I, Liu DD, Niu CW, Wen X, Yang GF, Xi Z (2017) Synthesis and herbicidal activity of pyrido 2,3-d pyrimidine-2,4-dione-benzoxazinone hybrids as protoporphyrinogen oxidase inhibitors. J Agric Food Chem 65:5278–5286

Wang DW, Zhang RB, Yu SY, Liang L, Ismail I, Li YH, Xu H, Wen X, Xi Z (2019) Discovery of novel N-isoxazolinylphenyltriazinones as promising protoporphyrinogen IX oxidase inhibitors. J Agric Food Chem 67:12382–12392

Wang MJ, Nan X, Feng G, Yu HT, Hu GF, Liu YQ (2014) Design, synthesis and bioactivity evaluation of novel acylthiourea derivatives of cantharidin. Ind Crop Prod 55:11–18

Yang R (2001) Advances on development of tetrahydrophthalimide herbicides. Pesticides 41:7–9

Ye F, Ma P, Zhang YY, Li P, Yang F, Fu Y (2018) Herbicidal activity and molecular docking study of novel accase inhibitors. Front Plant Sci 9:10

Ye F, Zhai Y, Guo KL, Liu YX, Li N, Gao S, Zhao LX, Fu Y (2019a) Safeners improve maize tolerance under herbicide toxicity stress by increasing the activity of enzymes in vivo. J Agric Food Chem 67:11568–11576

Ye F, Zhai Y, Kang T, Wu SL, Li JJ, Gao S, Zhao LX, Fu Y (2019b) Rational design, synthesis and structure-activity relationship of novel substituted oxazole isoxazole carboxamides as herbicide safener. Pest Biochem Physiol 157:60–68

Yu HB, Yang HB, Gui DL, Lv L, Li B (2011) Synthesis and herbicidal activity of diphenyl ether derivatives containing unsaturated carboxylates. J Agric Food Chem 59:11718–11726

Zhang YY, Gao S, Hoang MT, Wang ZW, Ma X, Zhai Y, Zhao LX, Fu Y, Ye F (2020a) Protective efficacy of novel phenoxyacetyl oxazolidine derivatives as safeners against nicosulfuron toxicity in maize. Pest Manag Sci, 10.1002/ps.6005

Zhang YY, Gao S, Liu YX, Wang C, Jiang W, Zhao LX, Fu Y, Ye F (2020b) Design, synthesis, and biological activity of novel diazabicyclo derivatives as safeners. J Agric Food Chem 68:3403–3414

Zhao LX, Jiang MJ, Hu JJ, Zou Y-L, Cheng Y, Ren T, Gao S, Fu Y, Ye F (2020) Design, synthesis, and herbicidal activity of novel diphenyl ether derivatives containing fast degrading tetrahydrophthalimide. J Agric Food Chem 68:3729–3741

https://doi.org/10.1017/wsc.2020.66 Published online by Cambridge University Press